Particle Swarm Optimization Based Analysis to Unlocking the Neutrino Mass Puzzle using $A_4 \times Z_3 \times Z_{10}$ Flavor Symmetry

M.W. Aslam,[a] **A.A. Zafar,**[a] **M.N. Aslam,**[b,d,e] **A.A Bhatti,**[c] **T. Hussain,**[c] and **M. Iqbal**[f]

[a]*Department of Physics, University of the Punjab,*
Lahore, Pakistan

[b]*Center for Mathematical Sciences (CMS), Pakistan Institute of Engineering & Applied Sciences,*
Nilore, 45650, Islamabad, Pakistan

[c]*Centre for High Energy Physics, University of the Punjab,*
Lahore, Pakistan

[d]*School of Mathematics, Minhaj University*
Lahore, Pakistan

[e]*Department of Physics and Applied Mathematics (DPAM), Pakistan Institute of Engineering &*
Applied Sciences,
Nilore, 45650, Islamabad, Pakistan

[f]*College of Statistical Sciences, University of the Punjab,*
Lahore, Pakistan

E-mail: waheed10aslam@gmail.com, waheed-979531@pu.edu.pk

ABSTRACT: New research has highlighted a shortfall in the Standard Model (SM) because it predicts neutrinos to have zero mass. However, recent experiments on neutrino oscillation have revealed that the majority of neutrino parameters indeed indicate their significant mass. In response, scientists are increasingly incorporating discrete symmetries alongside continuous ones for better justification of observed patterns of neutrino mixing. In this study, we have examined a model within $A_4 \times Z_3 \times Z_{10}$ symmetry to estimate the neutrino masses using particle swarm optimization technique for both mass hierarchy of neutrino. This model employed a hybrid seesaw mechanism, a combination of seesaw mechanism of type-I and type-II, to establish the effective Majorana neutrino mass matrix. After calculating the mass eigenvalues and lepton mixing matrix upto second order perturbation theory in this framework, this study seeks to investigate the scalar potential for vacuum expectation values (VEVs), optimize the parameters, U_{PMNS} matrix, neutrino masses: $|m_1'^N| = 0.0292794 - 0.0435082 \ eV$, $|m_2'^N| = 1.78893 \times 10^{-18} - 0.0293509 \ eV$, $—m_3'^N| = 0.0307414 - 0.0471467 \ eV$, $|m_1'^I| = 0.00982013 - 0.0453623 \ eV$, $|m_{2|}'^I = 0.0379702 - 0.0471197 \ eV$, and $|m_3'^I| = 0.0122063 - 0.027544 \ eV$, effective neutrino mass parameters: $\langle m_{ee} \rangle^N = (0.170 - 3.93) \times 10^{-2} \ eV$, $\langle m_\beta \rangle^N = (0.471 - 1.39) \times 10^{-2} \ eV$, $\langle m_{ee} \rangle^I = (1.85 - 4.55) \times 10^{-2} \ eV$ and $\langle m_\beta \rangle^I = (2.26 - 4.56) \times 10^{-2} \ eV$, are predicted for both mass hierarchy through particle swarm optimization (PSO), showing strong agreement with recent experimental findings.

KEYWORDS: Discrete symmetry, Neutrino mixing, Particle swarm optimization

Contents

1 Introduction

Known as the "ghost particles" of the universe, neutrinos have long intrigued the interest of cosmologists and physicists alike. Despite being among the most prevalent particles in the universe, these elementary particles (which are electrically neutral and almost massless) interact with matter very weakly, which makes them notoriously difficult to detect. In 1930, Wolfgang Pauli postulated the existence of neutrinos as a possible explanation for the violation of energy conservation observed in beta decay, they were only ever considered theoretical particles. Frederick Reines and Clyde Cowan eventually detected neutrinos in 1956 [1]. Neutrinos, in spite of their spectral appearance, are essential to the understanding of fundamental physics and the universe's evolution. Many astrophysical processes, such as nuclear fusion in stars [2], supernova explosions [3–7], and even the Big Bang itself [8, 9], produce them. Neutrinos are also essential for solving some of the most significant mysteries in cosmology and particle physics, including the properties of the elusive Higgs boson [10], the nature of dark matter [11–15], and the universe's imbalance between matter and antimatter [16]. One of the central puzzles surrounding neutrinos is their masses [17]. Neutrinos were originally thought to be massless in accordance with the SM of particle physics [18]. However, experiments in the late 20th and early 21st centuries, such as those conducted by the Super-Kamiokande [19], KamLAND [20], K2K [21], Fermilab-MINOS [22], Sudbury Neutrino Observatory collaborations [19] and CERN-OPERA [23] provided irrefutable evidence that neutrinos oscillate between different flavors (electron, muon, and tau), a phenomenon that can only occur if they possess non-zero masses. This discovery fundamentally challenged our understanding of neutrinos and underscored the need for new theoretical frameworks beyond the SM.

Researcher are looking in detail into seesaw frameworks, particularly type-I [24–28] and type-II [29–31], aside from several other methods to explain small neutrino masses. Majorana and Dirac mass terms derive from the introduction of extra right-handed neutrinos in SM in type I. Majorana mass terms derive from the introduction of heavy $SU(2)_L$ triplet in SM in type-II. A hybrid seesaw mechanism [24, 32, 33] has been proposed for improved mass suppression and new mixing patterns by combining type-I and type-II. With this hybrid technique, one may explore various lepton mixing scenarios and generate effective Majorana neutrino mass matrices.

Considering the recent discovery of non-zero, small neutrino masses in multiple neutrino oscillation experiments, numerous models for neutrino mass have been developed. These models are constructed based on different discrete symmetries such as S_3, S_4, A_4, A_5, $\Delta(27)$, T_7, T_{13} etc [34–52]. In the majority of cases, these models extend the Standard Model (SM) by incorporating the desired symmetries through the addition of specific field contents with their corresponding charges. These models postulate specific symmetries within the neutrino sector, leading to distinctive predictions for neutrino masses and mixing patterns. However, deriving expressions from these models often entails intricate mathematical formulations, posing challenges in their analytical solutions.

In these models, one of the prominent complications arises from the complexity of the equations. These equations typically involve nonlinear terms among the neutrino mass eigenstates. Solving such type of expressions analytically can be daunting, requiring sophisticated mathematical techniques and computational resources. In addressing these challenges, researchers have turned to computational methods to tackle the intricate expressions. Among these methods, One particularly effective method for handling challenging optimization problems is particle swarm optimization (PSO). The collective actions of fish and birds serve as the model for this population-based algorithm and metaheuristic approach. PSO is used for approximating parameters in different types of research problems [53, 54]. In 1995, Russell Eberhart and James Kennedy introduced the concept of PSO. [55–57], drawing inspiration from genetic algorithms (GAs) to refine its design [55]. PSO is commonly used to find optimal solutions to optimization problems, where the aim is to minimize or maximize a particular fitness function. PSO is versatile and has been utilized in diverse optimization scenarios, including engineering design [58–60], image processing [61–63], financial modeling [64–67] and neural network training [68, 69]. Its efficacy is further underscored by its widespread use in diverse optimization challenges, encompassing high-dimensional data clustering [70, 71], parameter estimation for chaotic maps [72, 73], optimization of core loading models in nuclear reactors [74], optimization of nonlinear reference frames [75], attainment of optimal reactive power distribution [76], as well as problem-solving in domains such as optical properties of multilayer thin films [77–80] and autoregressive models with moving average [81–83]. Additionally, PSO has proven effective in addressing challenges related to parameter estimation in electromagnetic plane waves [84]. Its simplicity, ease of implementation, and ability to handle non-linear and complex objective functions make it a popular choice for solving optimization problems. PSO stands out in particular for having an easy-to-implement architecture and requiring less memory [85, 86].

After calculating the mass eigenvalues and lepton mixing matrix upto second order perturbation theory in the framework [87] based on A_4 symmetry, this study seeks to investigate the minimization of the scalar potential for VEVs and optimize the parameters for U_{PMNS} matrix, neutrino masses and effective neutrino mass parameters: $\langle m_{ee} \rangle$, m_β, for both mass hierarchy through particle swarm optimization (PSO). The format of this article is as follows: The A_4 model is presented in the next section 2. In addition to describe the superpotential terms for charged leptons and neutrinos, subsection 2.1 provide the explanation for the mass eigenvalues and mixing matrix upto second order perturbation theory. Section 3 focuses on the utilization of PSO to determine optimal parameter values for computing neutrino masses. Section 4 presents the scalar potential invariant under $SU(2)_L \times A_4 \times Z_3 \times Z_{10}$, along with conditions for its minimization and explores the utilization of PSO in determining optimal parameter values for VEVs of the scalars. At the end, in section 5, we provide a conclusion of our research. We provide an explanation of the A_4 group in appendix A.

2   The A_4 based Model

In [87], they extended the SM group with A_4 symmetry with three right handed heavy singlet neutrino fields $(\nu_{e_R}, \nu_{\mu_R}, \nu_{\tau_R})$ and with seven scalars ϕ, Φ, η, κ, Δ, ξ, ξ'. The $SU(2)_L$ doublets ϕ, Φ and $SU(2)_L$ triplet Δ are taken as A_4 triplet. Four $SU(2)_L$ singlets η, κ, ξ and ξ' are taken as the singlets of A_4 as $1''$, $1'$, 1 and 1 respectively. Two additional symmetries, namely Z_3 and Z_{10} are also introduced to incorporate the undesired terms, where, Z_{10} refers to the symmetry of integers modulo 10. A summary of all the fields under $SU(2)_L$, A_4, Z_3 and Z_{10} are shown in table 1.

Fields	D_{l_L}	l_R	ν_{l_R}	ϕ	Φ	η	κ	Δ	ξ	ξ'
$SU(2)_L$	2	1	1	2	2	1	1	3	1	1
A_4	3	$(1, 1'', 1')$	$(1, 1'', 1')$	3	3	$1''$	$1'$	3	1	1
Z_3	1	(ω, ω, ω)	$(1, 1, 1)$	ω^2	1	1	1	1	1	1
Z_{10}	0	0	$(0, 4, 6)$	0	0	2	8	0	6	4

Table 1. The properties of transformation under $SU(2)_L \times A_4 \times Z_3 \times Z_{10}$.

2.1   Mass matrices of charged lepton and neutrino

The Lagrangian serves as a cornerstone in describing the interactions and behaviors of particles within the context of physics of particles. The superpotential term for charged leptons, Dirac neutrinos and right handed Majorana neutrinos is given as

$$
\begin{aligned}
-\mathcal{L}_Y =& y_e(\overline{D}_{l_L}\phi)e_R + y_\mu(\overline{D}_{l_L}\phi)\mu_R + y_\tau(\overline{D}_{l_L}\phi)\tau_R + y_1(\overline{D}_{l_L}\Phi)\nu_{e_R} + \frac{y_2}{\Lambda}(\overline{D}_{l_L}\Phi)\nu_{\mu_R}\xi \\
&+ \frac{y_3}{\Lambda}(\overline{D}_{l_L}\Phi)\nu_{\tau_R}\xi' + \frac{1}{2}M[(\overline{\nu_{e_R}^c}\nu_{e_R}) + (\overline{\nu_{\mu_R}^c}\nu_{\tau_R}) + (\overline{\nu_{\tau_R}^c}\nu_{\mu_R})] \\
&+ \frac{1}{2}y_R[(\overline{\nu_{\mu_R}^c}\nu_{\mu_R})\eta + (\overline{\nu_{\tau_R}^c}\nu_{\tau_R})\kappa] + y(\overline{D}_{l_L}D_{l_L}^c)i\tau^2\Delta + h.c,
\end{aligned}
\tag{2.1}
$$

in this context, y_e, y_μ and y_τ represent Yukawa couplings. Due to the VEVs (see section 4), one can generate mass matrices for charged leptons (M_l), Dirac neutrinos (M_D) and right handed Majorana neutrinos as

$$M_l = v \begin{pmatrix} y_e & 0 & 0 \\ 0 & y_\mu & 0 \\ 0 & 0 & y_\tau \end{pmatrix} \quad , \qquad M_D = u \begin{pmatrix} 0 & \frac{y_2 v_\epsilon}{\Lambda} & \frac{y_3 v_\epsilon}{\Lambda} \\ y_1 & 0 & \frac{y_3 v_\epsilon}{\Lambda} \\ y_1 & \frac{y_2 v_\epsilon}{\Lambda} & 0 \end{pmatrix}, \tag{2.2}$$

$$M_R = \begin{pmatrix} M & 0 & 0 \\ 0 & y_R v_m & M \\ 0 & M & y_R v_m \end{pmatrix}, \qquad M'' = \frac{y\omega}{3} \begin{pmatrix} 0 & 1 & -1 \\ 1 & 2 & 0 \\ -1 & 0 & -2 \end{pmatrix}. \tag{2.3}$$

Here, seesaw frameworks, particularly type-I [24–28] and type-II [29–31], used besides several other methods to explain small neutrino masses. Majorana and Dirac mass terms derived from the introduction of extra right-handed neutrinos in SM in type I. Majorana mass terms (M'') derived from the introduction of heavy $SU(2)_L$ triplet in SM in type-II. In other words, a hybrid seesaw mechanism [24, 32, 33] proposed for improved mass suppression and new mixing patterns by combining type-I and type-II. With this hybrid technique, one may explore various lepton mixing scenarios and generate effective Majorana neutrino mass matrices (M_ν) as

$$M_\nu = M' + M'' = -m_D M_R^{-1} m_D^T + M'' \tag{2.4}$$

with

$$M' = \begin{pmatrix} P & Q & Q \\ Q & R & S \\ Q & S & R \end{pmatrix}, \qquad M'' = \begin{pmatrix} 0 & p & -p \\ p & q & 0 \\ -p & 0 & -q \end{pmatrix},$$

$$p = \frac{y\omega}{3}, \quad q = 2p, \quad P = \frac{u^2 v_\epsilon^2 \left(\left(y_2^2 + y_3^2 \right) v_m y_R - 2 M y_2 y_3 \right)}{\Lambda^2 \left(M^2 - v_m^2 y_R^2 \right)},$$

$$Q = \frac{u^2 y_3 v_\epsilon^2 \left(y_3 v_m y_R - M y_2 \right)}{\Lambda^2 \left(M^2 - v_m^2 y_R^2 \right)}, \quad R = u^2 \left(\frac{y_3^2 v_m y_R v_\epsilon^2}{\Lambda^2 \left(M^2 - v_m^2 y_R^2 \right)} - \frac{y_1^2}{M} \right), \tag{2.5}$$

$$S = -\frac{M u^2 y_2 y_3 v_\epsilon^2}{\Lambda^2 \left(M^2 - v_m^2 y_R^2 \right)} - \frac{u^2 y_1^2}{M}.$$

The first matrix of effective Majorana is diagonalized by the subsequent mixing matrix,

$$U_0 = \begin{pmatrix} c & s & 0 \\ -s/\sqrt{2} & c/\sqrt{2} & 1/\sqrt{2} \\ -s/\sqrt{2} & c/\sqrt{2} & -1/\sqrt{2} \end{pmatrix}, \tag{2.6}$$

such as $diag(m_1, m_2, m_3) = U_0^T M_1 U_0$, where, $c = \cos\theta$, $s = \sin\theta$ and $\theta = Cos^{-1}(\frac{k}{\sqrt{k^2+2}})$ with,

$$k = \frac{P - R - S - \sqrt{P^2 - 2PR - 2PS + 8Q^2 + R^2 + 2RS + S^2}}{2Q}, \tag{2.7}$$

and

$$m_{1,2} = \frac{1}{2}(P + R + S \mp \sqrt{(-P + R + S)^2 + 8Q^2}), \qquad m_3 = R - S. \tag{2.8}$$

In the context of three-neutrino physics, the mixing matrix of lepton (U_{PMNS}) may be represented as [88]

$$U_{PMNS} = \begin{pmatrix} c_{12}c_{13} & s_{12}c_{13} & s_{13}e^{i\delta} \\ -s_{12}c_{23}-c_{12}s_{13}s_{23}e^{i\delta} & c_{12}c_{23}-s_{12}s_{13}s_{23}e^{i\delta} & c_{13}s_{23} \\ s_{12}s_{23}-c_{12}c_{23}s_{13}e^{i\delta} & -c_{12}s_{23}-s_{12}s_{13}c_{23}e^{i\delta} & c_{13}c_{23} \end{pmatrix} P_{12} \qquad (2.9)$$

where, $P_{12} = diag(1, e^{i\beta_1}, e^{i\beta_2})$ which contains two Majorana phases that do not influence neutrino oscillations. The matrix U_0 in equation 2.6 suggests $\theta_{23} = \pi/4$, $\theta_{13} = 0$ and $\theta_{12} = \theta$, Recent data contradicts this claim. However, the inclusion of the second matrix in equation 2.4 is expected to ameliorate this discrepancy. In first-order perturbation corrections, the second matrix in equation 2.4 doesn't affect the eigenvalues but it does influence the eigenvectors. Moving to second-order perturbation theory, This matrix contributes to the determination of both eigenvalues and eigenvectors. Consequently, the masses of neutrino upto the second order perturbation corrections can be expressed as:

$$m_1' = m_1 + \frac{p^2\Gamma_1{}^2}{m_1-m_3}, \quad m_2' = m_2 + \frac{p^2\Gamma_2{}^2}{m_2-m_3}, \quad m_3' = m_3 + p^2\left(\frac{2\Gamma_3{}^2}{m_3-m_1} + \frac{\Gamma_2{}^2}{m_3-m_2}\right),$$
$$(2.10)$$

where the parameters p, q, and $m_{1,2,3}$ are defined in equations 2.5 and 2.8, respectively. Subsequently, the resulting lepton mixing matrix is as follows:

$$U = U_0 + \Delta U + \Delta U' \qquad (2.11)$$

where U_0 is given by in equation 2.6, ΔU represents the mixing matrix corresponding to first-order corrections, and $\Delta U'$ represents the mixing matrix corresponding to second-order corrections. They have the following entries:

$$(\Delta U)_{11} = (\Delta U)_{12} = 0,$$

$$(\Delta U)_{13} = p\left(\frac{\Gamma_1\cos\theta}{m_3-m_1} + \frac{\Gamma_2\sin\theta}{m_3-m_2}\right),$$

$$(\Delta U)_{21} = -(\Delta U)_{31} = \frac{p\Gamma_3}{m_3-m_1}, \quad (\Delta U)_{32} = -(\Delta U)_{22} = \frac{\sqrt{2}\Gamma_2 p}{2(m_3-m_2)},$$

$$(\Delta U)_{23} = (\Delta U)_{33} = \frac{p\left((m_1-m_2)\Gamma_4 + 2(m_1+m_2-2m_3)\right)}{2\sqrt{2}(m_3-m_1)(m_2-m_3)},$$

$$(\Delta U')_{11} = \frac{p^2\Gamma_1}{2(m_1-m_3)^2}\left[-\cos\theta\Gamma_1 + \frac{2\sin\theta(m_1-m_3)\Gamma_2}{m_1-m_2}\right],$$

$$(\Delta U')_{12} = \frac{p^2\Gamma_2}{2(m_2-m_3)^2}\left[-\sin\theta\Gamma_2 - \frac{2\cos\theta(m_2-m_3)\Gamma_1}{m_1-m_2}\right], \quad (\delta U')_{13} = 0,$$

$$(\Delta U')_{21} = (\Delta U')_{31} = p^2\Gamma_1\left[\frac{\Gamma_5(3m_1-m_2-2m_3)+m_1+m_2-2m_3)}{2\sqrt{2}(m_1-m_2)(m_1-m_3)^2}\right],$$

$$(\Delta U')_{22} = (\Delta U')_{32} = -p^2\Gamma_2\left[\frac{\Gamma_5(m_1-3m_2+2m_3)+m_1+m_2-2m_3}{2\sqrt{2}(m_1-m_2)(m_2-m_3)^2}\right],$$

$$(\Delta U')_{23} = -(\Delta U')_{33} = \frac{-p^2}{2\sqrt{2}}\left[\frac{\Gamma_1{}^2}{(m_1-m_3)^2} + \frac{\Gamma_2{}^2}{(m_2-m_3)^2}\right],$$

with, $\Gamma_1 = -2\sin\theta + \sqrt{2}\cos\theta$, $\Gamma_2 = \sqrt{2}\sin\theta + 2\cos\theta$, $\Gamma_3 = \sqrt{2}\sin\theta - \cos\theta$, $\Gamma_4 = \sqrt{2}\sin 2\theta + 2\cos 2\theta$ and $\Gamma_5 = \cos 2\theta + \sqrt{2}\sin\theta\cos\theta$. The lepton mixing angles can be determined from equations 2.11 and 2.9, which define the mixing matrix of neutrino:

$$t_{12} = \frac{|U_{12}|}{|U_{11}|}, \quad t_{23} = \frac{|U_{23}|}{|U_{33}|}, \quad s_{13} = |U_{13}|, \tag{2.12}$$

with, $s_{ij} = \sin\theta_{ij}$, $c_{ij} = \cos\theta_{ij}$ and $t_{ij} = \tan\theta_{ij}$.

3 Numerical Analysis

Taking into consideration the latest experimental data [26], the mixing angles are measured as follows: The solar neutrino mixing angle, θ_{12}, is determined to be $34° \pm 1°$, the atmospheric neutrino mixing angle, θ_{23}, is found to be $42° \pm 3°$, and the reactor angle, θ_{13}, is measured to be $8.5° \pm 0.5°$. Additionally, the squared mass differences are determined as $\Delta m_{\text{sol}}^2 = m_2'^2 - m_1'^2 \approx 7.53 \times 10^{-5}$ eV^2 and $\Delta m_{\text{atm}}^2 = m_3'^2 - m_2'^2 \approx 2.453 \times 10^{-3}$ eV^2 ($\Delta m_{\text{atm}}^2 = m_3'^2 - m_2'^2 \approx -2.536 \times 10^{-3}$ eV^2) for normal (inverted) neutrino mass ordering [89]. The lower and upper bounds of Σm are constrained to 0.06 eV and 0.12 eV, respectively [90]. Utilizing equations 2.11 and 2.12, the objective or fitness function (ϵ) corresponding to these experimental constraints can be expressed as follows.

$$\epsilon = \epsilon_1 + \epsilon_2 + \epsilon_3 + \epsilon_4 + \epsilon_5 + \epsilon_6, \tag{3.1}$$

with,

$$\epsilon_1 = \left[m_2'^2 - m_1'^2 - \Delta\text{m}_{\text{sol}}^2\right]^2, \quad \epsilon_2 = \left[m_3'^2 - m_2'^2 - \Delta\text{m}_{\text{atm}}^2\right]^2, \quad \epsilon_3 = \left[\frac{|U_{12}|}{|U_{11}|} - t_{12}\right]^2,$$

$$\epsilon_4 = \left[\frac{|U_{23}|}{|U_{33}|} - t_{23}\right]^2, \quad \epsilon_5 = \left[U_{13}e^{i\delta} - s_{13}\right]^2,$$

$$\epsilon_6 = \left[|m_1'| + |m_2'| + |m_3'| - \begin{pmatrix} 0.12 \ eV, & \text{for upper bound limit} \\ 0.06 \ eV, & \text{for lower bound limit} \end{pmatrix}\right]^2,$$
$$\tag{3.2}$$

where, $m_{1,2,3}'$, U_{11}, U_{12}, U_{23}, U_{33}, U_{13} are given in equations 2.10 and 2.11.

We use PSO algorithm to optimize the objective or fitness functions ϵ for optimal values of parameters. In the usual way of doing particle swarm optimization (PSO), we treat each possible solution to a problem is represented as a moving point within the search space. These points form a group called a 'swarm', and they work together to check out the whole search area. Each point is assigned a unique score based on its efficacy in solving the problem. Initially, these points are randomly selected. Throughout each iteration, the positions and velocities of the points are updated based on their previous performance

based on its local P_{LB}^{x-1} and global P_{GB}^{x-1} positions. The basic rules for updating position and velocity of a point are given as,

$$v_i^x = wv_i^{t-1} + c_1 r_1 (P_{LB}^{x-1} - X_i^{x-1}) + c_2 r_2 (P_{GB}^{x-1} - X_i^{x-1}), \qquad (3.3)$$

$$X_i^x = X_i^{x-1} + v_i^{x-1}. \qquad (3.4)$$

In these rules, i goes from 1 to p, where p is just a integer telling us how many points there are. The weight 'w' and c_1 and c_2 are also integers that help to control how the points move. Also, the velocity gradually gets smaller as we keep looking around (between 0 and 1). The random numbers r_1 and r_2 are just there to add a bit of randomness. Finally, the velocity of the points is kept within certain limits so they don't go too fast or too slow.

The points traverse the search space by adapting their positions and velocities, drawing from their individual experiences and insights gained from neighboring points. The algorithm involves the following key steps:

1. Initialization: Commence by populating a set of points, assigning them random positions and velocities distributed throughout the exploration area.

2. Objective Assessment: Assess the fitness or objective function value for each point according to its present position.

3. Update Personal and Global Bests: Update the personal best position (Pbest) for each point based on its current fitness. Update the global best position (Gbest) considering the best position among all points.

4. Update Velocities and Positions: Adjust the velocity and position of each point using its current velocity, personal best, and global best positions.

5. Iteration: Continue steps 2 through 4 for a predetermined number of iterations or until reaching a convergence criterion.

   The generic flow chart PSO is given in figure 1.

To inspire the development of meta-heuristic optimization algorithms, we employed PSO technique to minimize the objective function for both mass hierarchy and for upper and lower bound limits of Σm. The objective function is minimized through PSO with 500 iteration are presented in figure 2 and corresponding values of p, θ, m_1, m_2 and m_3 are given in table 2, 3, 4 and 5.

Parameters	Optimal values	Parameters	Optimal values
p	-0.00379512	θ	$-2.55067\ rad$
m_1	0.0435296	m_2	-0.0281861
m_3	0.0459604		

Table 2. The optimal values of parameters p, θ, m_1, m_2, m_3, through PSO for upper bound limit of $\Sigma m = 0.12\ eV$ and normal mass hierarchy.
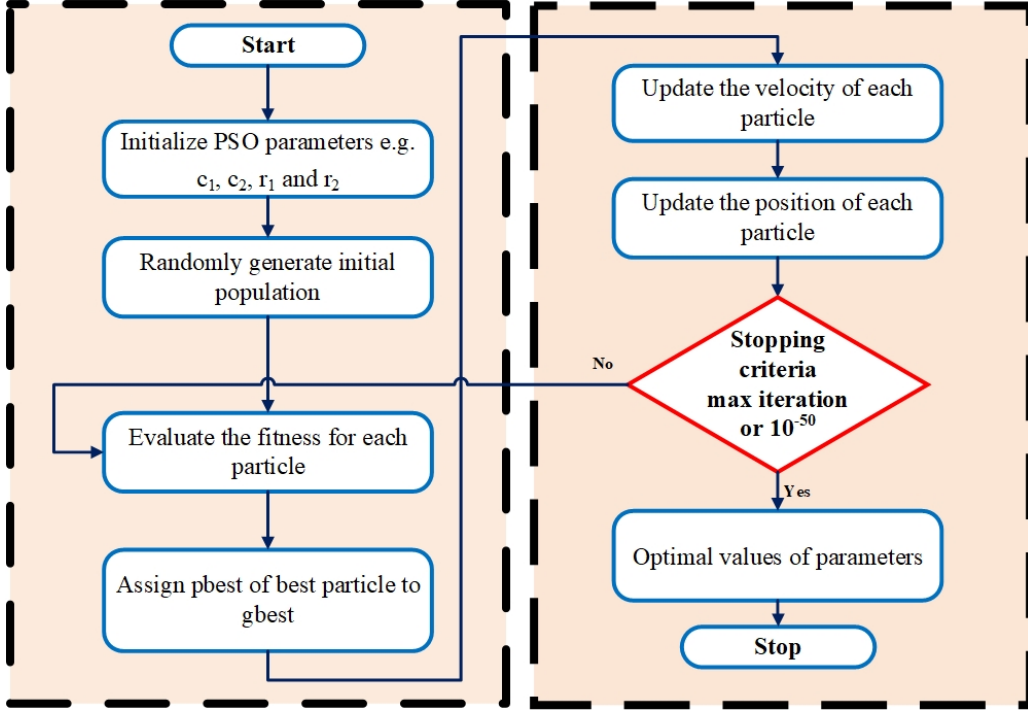
Figure 1. Generic flow chart of PSO

| Parameters	Optimal values	Parameters	Optimal values
p	-0.00152511	θ	$-5.69226\ rad$
m_1	0.029288	m_2	0.000468082
m_3	0.0302647		

Table 3. The optimal values of parameters p, θ, m_1, m_2, m_3, through PSO for lower bound limit of $\Sigma m = 0.06\ eV$ and normal mass hierarchy.

Parameters	Optimal values	Parameters	Optimal values
p	0.00290448	θ	$2.54093\ rad$
m_1	-0.0447439	m_2	0.0468078
m_3	0.0272375		

Table 4. The optimal values of parameters p, θ, m_1, m_2, m_3, through PSO for inverted mass hierarchy and for upper bound limit of $\Sigma m = 0.12\ eV$.

Parameters	Optimal values	Parameters	Optimal values
p	0.00248929	θ	$0.590928\ rad$
m_1	-0.00983418	m_2	0.0372062
m_3	-0.0114283		

Table 5. The optimal values of parameters p, θ, m_1, m_2, m_3, through PSO for lower bound limit of $\Sigma m = 0.06\ eV$ and inverted mass hierarchy.
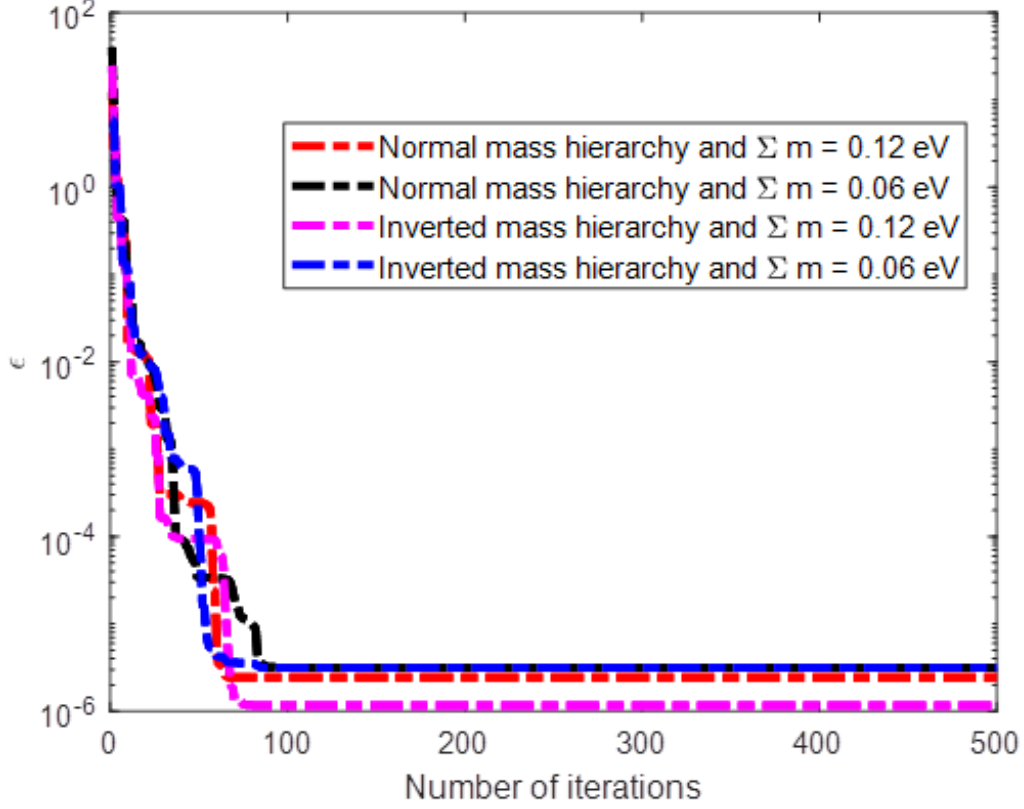
Figure 2. Fitness function versus number of iterations

The lepton mixing matrices upto second order perturbation theory for both mass hierarchy and for upper (0.12 eV) and lower (0.06 eV) bound limits of Σm are given as:

$$|U_{PMNS}^{(N)_{upper}}| = \begin{pmatrix} 0.819986 & 0.553082 & 0.14781 \\ 0.332956 & 0.671058 & 0.661831 \\ 0.465758 & 0.493805 & 0.735039 \end{pmatrix} \tag{3.5}$$

$$|U_{PMNS}^{(N)_{lower}}| = \begin{pmatrix} 0.819985 & 0.553085 & 0.14781 \\ 0.332958 & 0.671056 & 0.661831 \\ 0.465759 & 0.493804 & 0.735039 \end{pmatrix} \tag{3.6}$$

$$|U_{PMNS}^{(I)_{upper}}| = \begin{pmatrix} 0.820004 & 0.553096 & 0.147814 \\ 0.333852 & 0.671631 & 0.661835 \\ 0.464931 & 0.493097 & 0.735035 \end{pmatrix} \tag{3.7}$$

$$|U_{PMNS}^{(I)_{lower}}| = \begin{pmatrix} 0.819983 & 0.553087 & 0.147809 \\ 0.332959 & 0.671055 & 0.661832 \\ 0.46576 & 0.493803 & 0.735038 \end{pmatrix} \tag{3.8}$$

On the behalf of the values of p, θ, m_1, m_2 and m_3, the mass corrections upto second order perturbation theory for both mass hierarchy and for upper (0.12 eV) and lower

($0.06\ eV$) bound limits of Σm are given as: $|m_1'^{(N)upper}| = 0.0435082\ eV$, $|m_2'^{(N)upper}| = 0.0293509\ eV$, $|m_3'^{(N)upper}| = 0.0471467\ eV$, $|m_1'^{(N)lower}| = 0.0292794\ eV$, $|m_2'^{(N)lower}| = 1.78893 \times 10^{-18}\ eV$, $|m_3'^{(N)lower}| = 0.0307414\ eV$, $|m_1'^{(I)upper}| = 0.0453623\ eV$, $|m_2'^{(I)upper}| = 0.0471197\ eV$, $|m_3'^{(I)upper}| = 0.027544\ eV$, $|m_1'^{(I)lower}| = 0.00982013\ eV$, $|m_2'^{(I)lower}| = 0.0379702\ eV$ and $|m_3'^{(I)lower}| = 0.0122063\ eV$.

3.1 Effective neutrino mass parameters

The expressions for the effective neutrino masses [91–95] associated with neutrinoless double beta decay ($\langle m_{ee} \rangle$) and beta decay (m_β) are structured as follows:

$$m_\beta = \sqrt{\sum_{i=1}^{3} |U_{\text{ei}}|^2 m_i'^2}, \quad \langle m_{\text{ee}} \rangle = \left| \sum_{i=1}^{3} U_{\text{ei}}^2 m_i' \right|, \tag{3.9}$$

Considering the leptonic mixing matrix elements U_{ei} with i ranging from 1 to 3, representing the masses m_i' of three neutrinos, the effective neutrino masses associated with neutrinoless double beta decay ($\langle m_{ee} \rangle$) and beta decay (m_β) are computed using the parameters obtained in section 3. This calculation is performed for both mass hierarchy of neutrino, yielding the following results: $\langle m_{ee} \rangle^{(N)upper} = 3.93 \times 10^{-2}\ eV$, $\langle m_\beta \rangle^{(N)upper} = 1.39 \times 10^{-2}\ eV$, $\langle m_{ee} \rangle^{(N)lower} = 1.70 \times 10^{-3}\ eV$, $\langle m_\beta \rangle^{(N)lower} = 4.71 \times 10^{-3}\ eV$, $\langle m_{ee} \rangle^{(I)upper} = 4.55 \times 10^{-2}\ eV$, $\langle m_\beta \rangle^{(I)Upper} = 4.56 \times 10^{-2}\ eV$, $\langle m_{ee} \rangle^{(I)lower} = 1.85 \times 10^{-2}\ eV$ and $\langle m_\beta \rangle^{(I)lower} = 2.26 \times 10^{-2}\ eV$.

4 Vacuum alignment studies

In particle physics, the dynamics of scalar fields are encapsulated by an invariant scalar potential within the symmetry group. The following equation 4.1 describes the invariant scalar potential within the symmetry group $SU(2)_L \times A_4 \times Z_3 \times Z_{10}$. It plays a crucial role in understanding spontaneous symmetry breaking and the generation of particle masses. While A_4, Z_3, and Z_{10} are discrete symmetries that add to the rich structure of

the potential, the $SU(2)_L$ symmetry describes weak isospin.

$$
\begin{aligned}
V = &- \mu_\phi^2[\phi^\dagger\phi] + \lambda_1^\phi[\phi^\dagger\phi][\phi^\dagger\phi] + \lambda_2^\phi[\phi^\dagger\phi]_{1'}[\phi^\dagger\phi]_{1''} + \lambda_3^\phi[\phi^\dagger\phi]_{3_s}[\phi^\dagger\phi]_{3_s} + \lambda_4^\phi[\phi^\dagger\phi]_{3_s} \\
&[\phi^\dagger\phi]_{3_a} + \lambda_5^\phi[\phi^\dagger\phi]_{3_a}[\phi^\dagger\phi]_{3_a} - \mu_\Phi^2[\Phi^\dagger\Phi] + \lambda_1^\Phi[\Phi^\dagger\Phi][\Phi^\dagger\Phi] + \lambda_2^\Phi[\Phi^\dagger\Phi]_{1'}[\Phi^\dagger\Phi]_{1''} \\
&+ \lambda_3^\Phi[\Phi^\dagger\Phi]_{3_s}[\Phi^\dagger\Phi]_{3_s} + \lambda_4^\Phi[\Phi^\dagger\Phi]_{3_s}[\Phi^\dagger\Phi]_{3_a} + \lambda_5^\Phi[\Phi^\dagger\Phi]_{3_a}[\Phi^\dagger\Phi]_{3_a} - \mu_\Delta^2[\Delta^\dagger\Delta] \\
&+ \lambda_1^\Delta[\Delta^\dagger\Delta][\Delta^\dagger\Delta] + \lambda_2^\Delta[\Delta^\dagger\Delta]_{1'}[\Delta^\dagger\Delta]_{1''} + \lambda_3^\Delta[\Delta^\dagger\Delta]_{3_s}[\Delta^\dagger\Delta]_{3_s} + \lambda_4^\Delta[\Delta^\dagger\Delta]_{3_s} \\
&[\Delta^\dagger\Delta]_{3_a} + \lambda_5^\Delta[\Delta^\dagger\Delta]_{3_a}[\Delta^\dagger\Delta]_{3_a} + \lambda_1^{\phi\Phi}[\phi^\dagger\phi][\Phi^\dagger\Phi] + \lambda_2^{\phi\Phi}[[\phi^\dagger\phi]_{1'}[\Phi^\dagger\Phi]_{1''} + [\phi^\dagger\phi]_{1''} \\
&[\Phi^\dagger\Phi]_{1'}] + \lambda_3^{\phi\Phi}[\phi^\dagger\phi]_{3_s}[\Phi^\dagger\Phi]_{3_s} + \lambda_4^{\phi\Phi}[[\phi^\dagger\phi]_{3_s}[\Phi^\dagger\Phi]_{3_a} + [\phi^\dagger\phi]_{3_a}[\Phi^\dagger\Phi]_{3_s}] \\
&+ \lambda_5^{\phi\Phi}[\phi^\dagger\phi]_{3_a}[\Phi^\dagger\Phi]_{3_a} + \lambda_1^{\phi\Delta}[\phi^\dagger\phi][\Delta^\dagger\Delta] + \lambda_2^{\phi\Delta}[[\phi^\dagger\phi]_{1'}[\Delta^\dagger\Delta]_{1''} + [\phi^\dagger\phi]_{1''}[\Delta^\dagger\Delta]_{1'}] \\
&+ \lambda_3^{\phi\Delta}[\phi^\dagger\phi]_{3_s}[\Delta^\dagger\Delta]_{3_s} + \lambda_4^{\phi\Delta}[[\phi^\dagger\phi]_{3_s}[\Delta^\dagger\Delta]_{3_a} + [\phi^\dagger\phi]_{3_a}[\Delta^\dagger\Delta]_{3_s}] + \lambda_5^{\phi\Delta}[\phi^\dagger\phi]_{3_a} \\
&[\Delta^\dagger\Delta]_{3_a} + \lambda_1^{\Phi\Delta}[\Phi^\dagger\Phi][\Delta^\dagger\Delta] + \lambda_2^{\Phi\Delta}[[\Phi^\dagger\Phi]_{1'}[\Delta^\dagger\Delta]_{1''} + [\Phi^\dagger\Phi]_{1''}[\Delta^\dagger\Delta]_{1'}) \\
&+ \lambda_3^{\Phi\Delta}[\Phi^\dagger\Phi]_{3_s}[\Delta^\dagger\Delta]_{3_s} + \lambda_4^{\Phi\Delta}[[\Phi^\dagger\Phi]_{3_s}[\Delta^\dagger\Delta]_{3_a} + [\Phi^\dagger\Phi]_{3_a}[\Delta^\dagger\Delta]_{3_s}] + \lambda_5^{\Phi\Delta}[\Phi^\dagger\Phi]_{3_a} \\
&[\Delta^\dagger\Delta]_{3_a} - \mu_1^2[[\eta^\dagger\kappa] + [\kappa^\dagger\eta]] - \mu_2^2[[\eta\kappa] + [\kappa^\dagger\eta^\dagger]] + \lambda_1^{\eta\kappa}[\eta^\dagger\eta][\kappa^\dagger\kappa] - \mu_3^2[[\xi^\dagger\xi'] \\
&+ [\xi'^\dagger\xi]] - \mu_4^2[[\xi\xi'] + [\xi'^\dagger\xi^\dagger]] + \lambda_1^{\xi\xi'}[\xi^\dagger\xi][\xi'^\dagger\xi'].
\end{aligned}
\tag{4.1}
$$

The minimization conditions (VEVs) of this potential can result in the extreme solutions detailed in 4.2. These VEVs provide information about the stable configurations of the system since they represent crucial places where potential energy is minimized.

$$
\begin{aligned}
\langle\phi\rangle = v(1,0,0), \quad \langle\Delta\rangle = w(0,-1,1), \quad \langle\Phi\rangle = u(0,1,1), \\
\langle\eta\rangle = \langle\kappa\rangle = v_m, \quad \langle\xi\rangle = \langle\xi'\rangle = v_\epsilon,
\end{aligned}
\tag{4.2}
$$

with the conditions

$$
\frac{2}{3}u^2w\lambda_4^{\Phi\Delta} + \frac{2}{3}w^3\lambda_4^\Delta = 0,
\tag{4.3}
$$

$$
v_m^3\lambda_1^{\eta\kappa} - \mu_1^2v_m^3 - \mu_2^2v_m^3 = 0,
\tag{4.4}
$$

$$
\lambda_1^{\xi\xi'}v_\epsilon^3 - \mu_3^2v_\epsilon - \mu_4^2v_\epsilon = 0,
\tag{4.5}
$$

$$
2u^3\lambda_2^\Phi - \frac{8}{9}u^3\lambda_3^\Phi + 2uw^2\lambda_2^{\Phi\Delta} - \frac{4}{9}uw^2\lambda_3^{\Phi\Delta} = 0,
\tag{4.6}
$$

$$
2u^2v\lambda_1^{\phi\Phi} - \frac{4}{9}u^2v\lambda_3^{\phi\Phi} + 2v^3\lambda_1^\phi + \frac{8}{9}v^3\lambda_3^\phi - v\mu_\phi^2 - 2vw^2\lambda_1^{\phi\Delta} + \frac{4}{9}vw^2\lambda_3^{\phi\Delta} = 0,
\tag{4.7}
$$

$$
u^2v\lambda_2^{\phi\Phi} - \frac{2}{9}u^2v\lambda_3^{\phi\Phi} + \frac{1}{3}u^2v\lambda_4^{\phi\Phi} + vw^2\lambda_2^{\phi\Delta} - \frac{2}{9}vw^2\lambda_3^{\phi\Delta} + \frac{1}{3}vw^2\lambda_4^{\phi\Delta} = 0,
\tag{4.8}
$$

$$
u^2v\lambda_2^{\phi\Phi} - \frac{2}{9}u^2v\lambda_3^{\phi\Phi} - \frac{1}{3}u^2v\lambda_4^{\phi\Phi} + vw^2\lambda_2^{\phi\Delta} - \frac{2}{9}vw^2\lambda_3^{\phi\Delta} - \frac{1}{3}vw^2\lambda_4^{\phi\Delta} = 0,
\tag{4.9}
$$

$$
\begin{aligned}
&4u^3\lambda_1^\Phi + u^3\lambda_2^\Phi + \frac{4}{3}u^3\lambda_3^\Phi + \frac{1}{3}u^3\lambda_4^\Phi - u\mu_\Phi^2 + uv^2\lambda_1^{\phi\Phi} - \frac{2}{9}uv^2\lambda_3^{\phi\Phi} - \frac{1}{3}uv^2\lambda_4^{\phi\Phi} \\
&- 2uw^2\lambda_1^{\Phi\Delta} + uw^2\lambda_2^{\Phi\Delta} + \frac{2}{9}uw^2\lambda_3^{\Phi\Delta} - \frac{1}{3}uw^2\lambda_4^{\Phi\Delta} = 0,
\end{aligned}
\tag{4.10}
$$

$$
\begin{aligned}
&4u^3\lambda_1^\Phi + u^3\lambda_2^\Phi + \frac{4}{3}u^3\lambda_3^\Phi - \frac{1}{3}u^3\lambda_4^\Phi - u\mu_\Phi^2 + uv^2\lambda_1^{\phi\Phi} - \frac{2}{9}uv^2\lambda_3^{\phi\Phi} + \frac{1}{3}uv^2\lambda_4^{\phi\Phi} \\
&- 2uw^2\lambda_1^{\Phi\Delta} + uw^2\lambda_2^{\Phi\Delta} + \frac{2}{9}uw^2\lambda_3^{\Phi\Delta} + \frac{1}{3}uw^2\lambda_4^{\Phi\Delta} = 0,
\end{aligned}
\tag{4.11}
$$

$$2u^2w\lambda_1^{\Phi\Delta} - u^2w\lambda_2^{\Phi\Delta} - \frac{2}{9}u^2w\lambda_3^{\Phi\Delta} + \frac{1}{3}u^2w\lambda_4^{\Phi\Delta} + v^2w\lambda_1^{\phi\Delta} - \frac{2}{9}v^2w\lambda_3^{\phi\Delta} - \frac{1}{3}v^2w\lambda_4^{\phi\Delta}$$
$$- 4w^3\lambda_1^{\Delta} - w^3\lambda_2^{\Delta} - \frac{4}{3}w^3\lambda_3^{\Delta} - \frac{1}{3}w^3\lambda_4^{\Delta} - w\mu_\Delta^2 = 0, \tag{4.12}$$

$$- 2u^2w\lambda_1^{\Phi\Delta} + u^2w\lambda_2^{\Phi\Delta} + \frac{2}{9}u^2w\lambda_3^{\Phi\Delta} + \frac{1}{3}u^2w\lambda_4^{\Phi\Delta} - v^2w\lambda_1^{\phi\Delta} + \frac{2}{9}v^2w\lambda_3^{\phi\Delta} - \frac{1}{3}v^2w\lambda_4^{\phi\Delta}$$
$$+ 4w^3\lambda_1^{\Delta} + w^3\lambda_2^{\Delta} + \frac{4}{3}w^3\lambda_3^{\Delta} - \frac{1}{3}w^3\lambda_4^{\Delta} + w\mu_\Delta^2 = 0, \tag{4.13}$$

PSO Treatment for Scalar Potential:

Due to VEVs 4.2 and multiplication rules for A_4 symmetry given in A, equation 4.1 become as

$$V = -\mu_\phi^2 v^2 + \lambda_1^\phi v^4 + \frac{4}{9}\lambda_3^\phi v^4 - 2\mu_\Phi^2 u^2 + 4\lambda_1^\Phi u^4 + \lambda_2^\Phi u^4 + \frac{12}{9}\lambda_3^\Phi u^4 + 2\mu_\Delta^2 w^2 + 4\lambda_1^\Delta w^4$$
$$+ \lambda_2^\Delta w^4 + \frac{12}{9}\lambda_3^\Delta w^4 + 2\lambda_1^{\phi\Phi} v^2 u^2 - \frac{4}{9}\lambda_3^{\phi\Phi} v^2 u^2 - 2\lambda_1^{\phi\Delta} v^2 w^2 + \frac{4}{9}\lambda_3^{\phi\Delta} v^2 w^2 - 4\lambda_1^{\Phi\Delta} u^2 w^2$$
$$+ 2\lambda_2^{\Phi\Delta} u^2 w^2 + \frac{4}{9}\lambda_3^{\Phi\Delta} u^2 w^2 - 2\mu_1^2 v_m^2 - 2\mu_2^2 v_m^2 + \lambda_1^{\eta\kappa} v_m^4 - 2\mu_3^2 v_\epsilon^2 - 2\mu_4^2 v_\epsilon^2 + \lambda_1^{\xi\xi'} v_\epsilon^4, \tag{4.14}$$

and the fitness function (ϵ') for 4.14 is expressed as follows.

$$\epsilon' = \Bigg[-\mu_\phi^2 v^2 + \lambda_1^\phi v^4 + \frac{4}{9}\lambda_3^\phi v^4 - 2\mu_\Phi^2 u^2 + 4\lambda_1^\Phi u^4 + \lambda_2^\Phi u^4 + \frac{12}{9}\lambda_3^\Phi u^4 + 2\mu_\Delta^2 w^2 + 4\lambda_1^\Delta w^4$$
$$+ \lambda_2^\Delta w^4 + \frac{12}{9}\lambda_3^\Delta w^4 + 2\lambda_1^{\phi\Phi} v^2 u^2 - \frac{4}{9}\lambda_3^{\phi\Phi} v^2 u^2 - 2\lambda_1^{\phi\Delta} v^2 w^2 + \frac{4}{9}\lambda_3^{\phi\Delta} v^2 w^2 - 4\lambda_1^{\Phi\Delta} u^2 w^2$$
$$+ 2\lambda_2^{\Phi\Delta} u^2 w^2 + \frac{4}{9}\lambda_3^{\Phi\Delta} u^2 w^2 - 2\mu_1^2 v_m^2 - 2\mu_2^2 v_m^2 + \lambda_1^{\eta\kappa} v_m^4 - 2\mu_3^2 v_\epsilon^2 - 2\mu_4^2 v_\epsilon^2 + \lambda_1^{\xi\xi'} v_\epsilon^4 \Bigg]^2, \tag{4.15}$$

To stimulate the advancement of meta-heuristic optimization algorithms, we again utilized PSO technique to minimize the scalar potential. The objective function is minimized through PSO for scalar potential with 500 iteration is presented in figure 3. This figure demonstrates that the objective function converges to zero with each iteration when employing the VEVs provided in 4.2. The optimal parameter values, as measured within the objective function of the scalar potential using PSO technique, are listed in 6. The scalar potential is minimized from these optimal values.

5 Conclusion

In this study, we have examined a model within $A_4 \times Z_3 \times Z_{10}$ to estimate the neutrino masses using particle swarm optimization technique for both neutrino hierarchy. In this model, a hybrid seesaw mechanism proposed for improved mass suppression and new mixing patterns by combining type-I and type-II and generate effective Majorana neutrino mass matrices. After calculating the mass eigenvalues and lepton mixing matrix upto second order perturbation theory in the framework based on A_4 symmetry, we investigated the minimization of the scalar potential for VEVs through PSO. The utilization of PSO in determining optimal parameters for computing U_{PMNS} matrices,
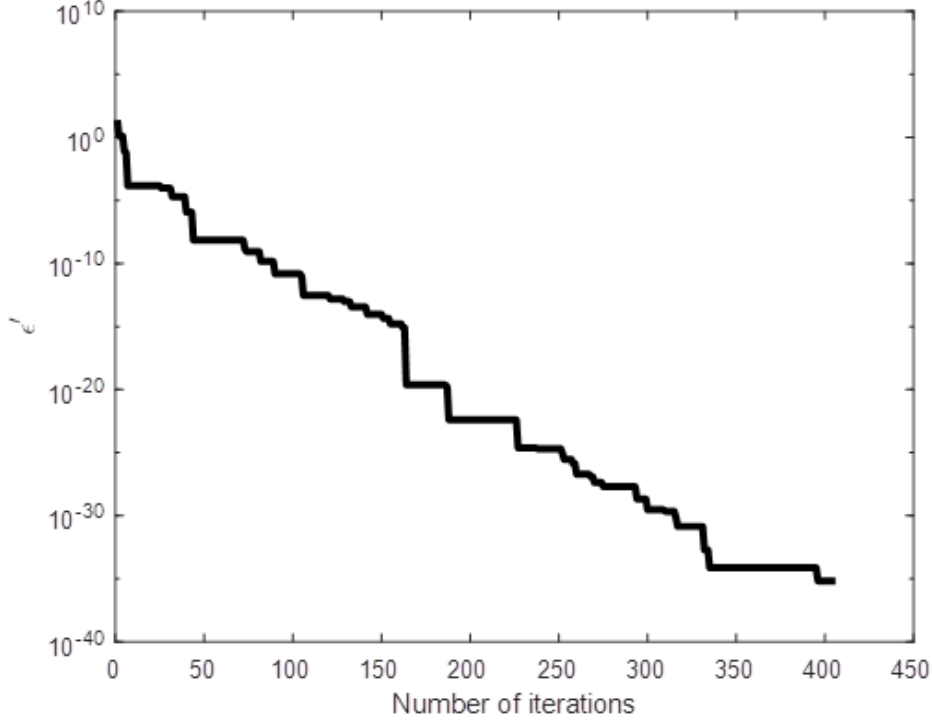
Figure 3. Fitness function of scalar potential versus number of iterations

Parameters	Optimal values	Parameters	Optimal values
μ_ϕ	0.47937	μ_Φ	4.0982
μ_Δ	1.59123	μ_1	-2.06518
μ_2	-5.15994	μ_3	-1.86719
μ_4	-0.0301591	λ_1^ϕ	-0.494641
λ_3^ϕ	0.965018	λ_1^Φ	3.54296
λ_2^Φ	-0.677823	λ_3^Φ	3.07826
λ_1^Δ	4.33307	λ_2^Δ	-6.61388
λ_3^Δ	1.96668	$\lambda_1^{\phi\Phi}$	4.87709
$\lambda_3^{\phi\Phi}$	-0.379146	$\lambda_1^{\phi\Delta}$	1.46855
$\lambda_3^{\phi\Delta}$	-1.76377	$\lambda_1^{\Phi\Delta}$	4.33631
$\lambda_2^{\Phi\Delta}$	2.62704	$\lambda_3^{\Phi\Delta}$	4.08727
$\lambda_1^{\eta\kappa}$	4.82545	$\lambda_1^{\xi\xi'}$	-0.412121
v	-2.42962	u	-0.913621
w	-1.19017	v_m	0.564846
v_ϵ	-0.363201		

Table 6. The optimal values of parameters given in 4.1 through PSO.

neutrino masses as: $|m_1'^N| = 0.0292794 - 0.0435082\ eV$, $|m_2'^N| = 1.78893 \times 10^{-18} - 0.0293509\ eV$, $|m_3'^N| = 0.0307414 - 0.0471467\ eV$, $|m_1'^I| = 0.00982013 - 0.0453623\ eV$, $|m_2'^I| = 0.0379702 - 0.0471197\ eV$, and $|m_3'^I| = 0.0122063 - 0.027544\ eV$, effective neutrino mass parameters as: $\langle m_{ee} \rangle^N = (0.170 - 3.93) \times 10^{-2}\ eV$, $\langle m_\beta \rangle^N = (0.471 - 1.39) \times 10^{-2}\ eV$, $\langle m_{ee} \rangle^I = (1.85 - 4.55) \times 10^{-2}\ eV$ and $\langle m_\beta \rangle^I = (2.26 - 4.56) \times 10^{-2}\ eV$ for both mass hierarchy are illustrated as well.

A A_4 group

The group A_4 [96] comprises all even permutations of S_4, resulting in an order of $(4!)/2 = 12$, with 12 different elements. A_4 is a tetrahedron symmetry group. A_4 notably exhibits isomorphism with $\Delta(12) \simeq (Z_2 \times Z_2) \rtimes Z_3$. There are four irreducible representations as there are four conjugacy classes. A_4 contains three singlets designated as $\mathbf{1}$, $\mathbf{1'}$, $\mathbf{1''}$ and one triplet, designated as $\mathbf{3}$.

The multiplication of triplets are given as

$$
\begin{pmatrix} j_1 \\ j_2 \\ k_3 \end{pmatrix}_{\mathbf{3}} \otimes \begin{pmatrix} k_1 \\ k_2 \\ k_3 \end{pmatrix}_{\mathbf{3}} = (j_1 k_1 + j_2 k_3 + j_3 k_2)_{\mathbf{1}} \oplus (j_3 k_3 + j_1 k_2 + j_2 k_1)_{\mathbf{1'}}
$$
$$
\oplus (j_2 k_2 + j_1 k_3 + j_3 k_1)_{\mathbf{1''}} \tag{A.1}
$$
$$
\oplus \frac{1}{3} \begin{pmatrix} 2j_1 k_1 - j_2 k_3 - j_3 k_2 \\ 2j_3 k_3 - j_1 k_2 - j_2 k_1 \\ 2j_2 k_2 - j_1 k_3 - j_3 k_1 \end{pmatrix}_{\mathbf{3_s}} \oplus \frac{1}{2} \begin{pmatrix} j_2 k_3 - j_3 k_2 \\ j_1 k_2 - j_2 k_1 \\ j_1 k_3 - j_3 k_1 \end{pmatrix}_{\mathbf{3_a}} .
$$

References

[1] C.L. Cowan, F. Reines, F.B. Harrison, H.W. Kruse and A.D. McGuire, *Detection of the free neutrino: A Confirmation*, *Science* **124** (1956) 103.

[2] G.G. Raffelt, *Neutrinos and stars*, `1201.1637`.

[3] A. Burrows, *Neutrinos From Supernova Explosions*, *Ann. Rev. Nucl. Part. Sci.* **40** (1990) 181.

[4] I. Tamborra and K. Murase, *Neutrinos from Supernovae*, *Space Sci. Rev.* **214** (2018) 31.

[5] A. Burrows and T. Young, *Neutrinos and supernova theory*, *Phys. Rept.* **333** (2000) 63.

[6] J. Cooperstein, *Neutrinos in Supernovae*, *Phys. Rept.* **163** (1988) 95.

[7] M. Herant, S.A. Colgate, W. Benz and C. Fryer, *Neutrinos and supernovae*, *Los Alamos Science* **25** (1997) 64.

[8] S. Sarkar, *Neutrinos from the Big Bang*, *arXiv e-prints* (2003) hep [`hep-ph/0302175`].

[9] G. Steigman, *Neutrinos and Big Bang Nucleosynthesis*, *Physica Scripta Volume T* **121** (2005) 142 [`hep-ph/0501100`].

[10] S. Chakraborty and S. Roy, *Higgs boson mass, neutrino masses and mixing and keV dark matter in an U(1)$_R$ - lepton number model*, *Journal of High Energy Physics* **2014** (2014) 101 [`1309.6538`].

[11] M. Blennow, M. Carrigan and E. Fernandez Martinez, *Probing the Dark Matter mass and nature with neutrinos*, *Journal of Cosmology and Astroparticle Physics* **2013** (2013) 038 [1303.4530].

[12] S.K. Agarwalla, M. Blennow, E. Fernandez Martinez and O. Mena, *Neutrino Probes of the Nature of Light Dark Matter*, *JCAP* **09** (2011) 004 [1105.4077].

[13] S. Dodelson and L.M. Widrow, *Sterile neutrinos as dark matter*, *Physical Review Letters* **72** (1994) 17 [hep-ph/9303287].

[14] G. Bertone and T. Tait, M. P., *A new era in the search for dark matter*, *Nature* **562** (2018) 51 [1810.01668].

[15] D. Hooper and E.A. Baltz, *Strategies for Determining the Nature of Dark Matter*, *Ann. Rev. Nucl. Part. Sci.* **58** (2008) 293 [0802.0702].

[16] T2K collaboration, *Constraint on the matter–antimatter symmetry-violating phase in neutrino oscillations*, *Nature* **580** (2020) 339 [1910.03887].

[17] C. Weinheimer and K. Zuber, *Neutrino Masses*, *Annalen Phys.* **525** (2013) 565 [1307.3518].

[18] S. Bilenky, *Introduction to the Physics of Massive and Mixed Neutrinos*, vol. 947, Springer (2018), 10.1007/978-3-319-74802-3.

[19] Y. Fukuda, T. Hayakawa, E. Ichihara, K. Inoue, K. Ishihara, H. Ishino et al., *Evidence for Oscillation of Atmospheric Neutrinos*, *Physical Review Letters* **81** (1998) 1562 [hep-ex/9807003].

[20] K. Eguchi, S. Enomoto, K. Furuno, J. Goldman, H. Hanada, H. Ikeda et al., *First Results from KamLAND: Evidence for Reactor Antineutrino Disappearance*, *Physical Review Letters* **90** (2003) 021802 [hep-ex/0212021].

[21] M.H. Ahn, E. Aliu, S. Andringa, S. Aoki, Y. Aoyama, J. Argyriades et al., *Measurement of neutrino oscillation by the K2K experiment*, *Physical Review D* **74** (2006) 072003 [hep-ex/0606032].

[22] D.G. Michael, P. Adamson, T. Alexopoulos, W.W.M. Allison, G.J. Alner, K. Anderson et al., *Observation of Muon Neutrino Disappearance with the MINOS Detectors in the NuMI Neutrino Beam*, *Physical Review Letters* **97** (2006) 191801 [hep-ex/0607088].

[23] R. Acquafredda, T. Adam, N. Agafonova, P. Alvarez Sanchez, M. Ambrosio, A. Anokhina et al., *The OPERA experiment in the CERN to Gran Sasso neutrino beam*, *Journal of Instrumentation* **04** (2009) 04018.

[24] Y. Cai, T. Han, T. Li and R. Ruiz, *Lepton Number Violation: Seesaw Models and Their Collider Tests*, *Front. in Phys.* **6** (2018) 40 [1711.02180].

[25] R.N. Mohapatra, *Seesaw mechanism and its implications*, hep-ph/0412379.

[26] S.F. King and C. Luhn, *Neutrino mass and mixing with discrete symmetry*, *Reports on Progress in Physics* **76** (2013) 056201 [1301.1340].

[27] R.N. Mohapatra and A.Y. Smirnov, *Neutrino Mass and New Physics*, *Ann. Rev. Nucl. Part. Sci.* **56** (2006) 569 [hep-ph/0603118].

[28] S.F. King, *Neutrino mass models*, *Rept. Prog. Phys.* **67** (2004) 107 [hep-ph/0310204].

[29] A. Melfo, M. Nemevšek, F. Nesti, G. Senjanović and Y. Zhang, *Type II neutrino seesaw mechanism at the LHC: The roadmap*, *Physical Review D* **85** (2012) 055018 [1108.4416].

[30] P. Fileviez Perez, T. Han, G.-y. Huang, T. Li and K. Wang, *Neutrino Masses and the CERN LHC: Testing Type II Seesaw*, *Phys. Rev. D* **78** (2008) 015018 [`0805.3536`].

[31] T.P. Cheng and L.-F. Li, *Neutrino Masses, Mixings and Oscillations in SU(2) × U(1) Models of Electroweak Interactions*, *Phys. Rev. D* **22** (1980) 2860.

[32] E.K. Akhmedov and M. Frigerio, *Interplay of type I and type II seesaw contributions to neutrino mass*, *Journal of High Energy Physics* **2007** (2007) 043 [`hep-ph/0609046`].

[33] C.-F. Wong and Y. Chen, *Tree level Majorana neutrino mass from Type-1 × Type-2 Seesaw mechanism with Dark Matter*, *Physics Letters B* **833** (2022) 137354 [`2205.08531`].

[34] M. Hirsch, S. Morisi and J.W.F. Valle, *A_4-based tri-bimaximal mixing within inverse and linear seesaw schemes*, *Physics Letters B* **679** (2009) 454 [`0905.3056`].

[35] A.E.C. Hernández, S. Kovalenko, H.N. Long and I. Schmidt, *A variant of 3-3-1 model for the generation of the SM fermion mass and mixing pattern*, *Journal of High Energy Physics* **2018** (2018) 144 [`1705.09169`].

[36] A.E. Cárcamo Hernández, I. de Medeiros Varzielas, M.L. López-Ibáñez and A. Melis, *Controlled fermion mixing and FCNCs in a $\Delta(27)$ 3+1 Higgs Doublet Model*, *Journal of High Energy Physics* **2021** (2021) 215 [`2102.05658`].

[37] M. Sruthilaya, R. Mohanta and S. Patra, *A_4 realization of linear seesaw and neutrino phenomenology*, *European Physical Journal C* **78** (2018) 719 [`1709.01737`].

[38] D. Borah and B. Karmakar, *Linear seesaw for Dirac neutrinos with A_4 flavour symmetry*, *Physics Letters B* **789** (2019) 59 [`1806.10685`].

[39] A.E.C. Hernández, K.N. Vishnudath and J.W.F. Valle, *Linear seesaw mechanism from dark sector*, *Journal of High Energy Physics* **2023** (2023) 46 [`2305.02273`].

[40] C. Luhn, S. Nasri and P. Ramond, *Tri-bimaximal neutrino mixing and the family symmetry $Z_7 \rtimes Z_3$*, *Physics Letters B* **652** (2007) 27 [`0706.2341`].

[41] C. Hagedorn, M.A. Schmidt and A.Y. Smirnov, *Lepton mixing and cancellation of the Dirac mass hierarchy in SO(10) GUTs with flavor symmetries T_7 and $\Sigma(81)$*, *Physical Review D* **79** (2009) 036002 [`0811.2955`].

[42] Q.-H. Cao, S. Khalil, E. Ma and H. Okada, *Observable T_7 Lepton Flavor Symmetry at the Large Hadron Collider*, *Physical Review Letters* **106** (2011) 131801 [`1009.5415`].

[43] C. Luhn, K.M. Parattu and A. Wingerter, *A minimal model of neutrino flavor*, *Journal of High Energy Physics* **2012** (2012) 96 [`1210.1197`].

[44] Y. Kajiyama, H. Okada and K. Yagyu, *T_7 flavor model in three loop seesaw and Higgs phenomenology*, *Journal of High Energy Physics* **2013** (2013) 196 [`1307.0480`].

[45] C. Bonilla, S. Morisi, E. Peinado and J.W.F. Valle, *Relating quarks and leptons with the T_7 flavour group*, *Physics Letters B* **742** (2015) 99 [`1411.4883`].

[46] V.V. Vien and H.N. Long, *The T_7 flavor symmetry in 3-3-1 model with neutral leptons*, *Journal of High Energy Physics* **2014** (2014) 133 [`1402.1256`].

[47] V.V. Vien, *T_7 flavor symmetry scheme for understanding neutrino mass and mixing in 3-3-1 model with neutral leptons*, *Modern Physics Letters A* **29** (2014) 1450139 [`1508.02585`].

[48] A.E. Cárcamo Hernández and R. Martinez, *Fermion mass and mixing pattern in a minimal T_7 flavor 331 model*, *Journal of Physics G: Nuclear and Particle Physics* **43** (2016) 45003 [`1511.07997`].

[49] C. Arbeláez, A.E. Cárcamo Hernández, S. Kovalenko and I. Schmidt, *Adjoint S U (5) GUT model with T_7 flavor symmetry*, *Physical Review D* **92** (2015) 115015 [1507.03852].

[50] G.-J. Ding, *Tri-bimaximal neutrino mixing and the T flavor symmetry*, *Nuclear Physics B* **853** (2011) 635 [1105.5879].

[51] C. Hartmann, *Frobenius group T_{13} and the canonical seesaw mechanism applied to neutrino mixing*, *Physical Review D* **85** (2012) 013012 [1109.5143].

[52] V.V. Vien and H.N. Long, *Fermion Mass and Mixing in a Simple Extension of the Standard Model Based on T_7 Flavor Symmetry*, *Physics of Atomic Nuclei* **82** (2019) 168.

[53] R. Toushmalani, *Gravity inversion of a fault by Particle swarm optimization (PSO)*, *SpringerPlus* **2** (2013) 1.

[54] S. Bassi, M. Mishra and E. Omizegba, *Automatic tuning of proportional-integral-derivative (PID) controller using particle swarm optimization (PSO) algorithm*, *International Journal of Artificial Intelligence & Applications* **2** (2011) 25.

[55] S. Panda and N.P. Padhy, *Comparison of particle swarm optimization and genetic algorithm for FACTS-based controller design*, *Applied soft computing* **8** (2008) 1418.

[56] M.O. Okwu, L.K. Tartibu, M.O. Okwu and L.K. Tartibu, *Particle swarm optimisation*, *Metaheuristic Optimization: Nature-Inspired Algorithms Swarm and Computational Intelligence, Theory and Applications* (2021) 5.

[57] Y. Yu and S. Yin, *A Comparison between Generic Algorithm and Particle Swarm Optimization*, .

[58] N.B. Guedria, *Improved accelerated PSO algorithm for mechanical engineering optimization problems*, *Applied Soft Computing* **40** (2016) 455.

[59] A. Kaveh and E.A. NASR, *Engineering design optimization using a hybrid PSO and HS algorithm*, .

[60] N. Kumar, S.K. Mahato and A.K. Bhunia, *Design of an efficient hybridized CS-PSO algorithm and its applications for solving constrained and bound constrained structural engineering design problems*, *Results in Control and Optimization* **5** (2021) 100064.

[61] S. Djemame, M. Batouche, H. Oulhadj and P. Siarry, *Solving reverse emergence with quantum PSO application to image processing*, *Soft Computing* **23** (2019) 6921.

[62] R.P. Singh, M. Dixit and S. Silakari, *Image contrast enhancement using GA and PSO: a survey*, .

[63] J. Pramanik, S. Dalai and D. Rana, *Image registration using PSO and APSO: a comparative analysis*, *International Journal of Computer Applications* **116** (2015) .

[64] F.Z. Azayite and S. Achchab, *Financial Early Warning System Model Based on Neural Networks, PSO and SA Algorithms*, .

[65] S.C. Chiam, K.C. Tan and A.A. Mamun, *A memetic model of evolutionary PSO for computational finance applications*, *Expert Systems with Applications* **36** (2009) 3695.

[66] Y. Pan et al., *Design of financial management model using the forward neural network based on particle swarm optimization algorithm*, *Computational Intelligence and Neuroscience* **2022** (2022) .

[67] Y. Marinakis, M. Marinaki, M. Doumpos and C. Zopounidis, *Ant colony and particle swarm optimization for financial classification problems*, Expert Systems with Applications **36** (2009) 10604.

[68] M. Meissner, M. Schmuker and G. Schneider, *Optimized Particle Swarm Optimization (OPSO) and its application to artificial neural network training*, BMC bioinformatics **7** (2006) 1.

[69] H.T. Rauf, W.H. Bangyal, J. Ahmad and S.A. Bangyal, *Training of artificial neural network using pso with novel initialization technique*, .

[70] A.A. Esmin, R.A. Coelho and S. Matwin, *A review on particle swarm optimization algorithm and its variants to clustering high-dimensional data*, Artificial Intelligence Review **44** (2015) 23.

[71] S. Rana, S. Jasola and R. Kumar, *A review on particle swarm optimization algorithms and their applications to data clustering*, Artificial Intelligence Review **35** (2011) 211.

[72] Q. He, L. Wang and B. Liu, *Parameter estimation for chaotic systems by particle swarm optimization*, Chaos, Solitons & Fractals **34** (2007) 654.

[73] B. Alatas, E. Akin and A.B. Ozer, *Chaos embedded particle swarm optimization algorithms*, Chaos, Solitons & Fractals **40** (2009) 1715.

[74] D. Babazadeh, M. Boroushaki and C. Lucas, *Optimization of fuel core loading pattern design in a VVER nuclear power reactors using Particle Swarm Optimization (PSO)*, Annals of nuclear energy **36** (2009) 923.

[75] A.M. Ibrahim and M.A. Tawhid, *A hybridization of cuckoo search and particle swarm optimization for solving nonlinear systems*, Evolutionary Intelligence **12** (2019) 541.

[76] P. Subbaraj and P. Rajnarayanan, *Hybrid particle swarm optimization based optimal reactive power dispatch*, International Journal of Computer Applications **1** (2010) 65.

[77] A. Jiang, Y. Osamu and L. Chen, *Multilayer optical thin film design with deep Q learning*, Scientific reports **10** (2020) 12780.

[78] C. Yue, Z. Qin, Y. Lang and Q. Liu, *Determination of thin metal film's thickness and optical constants based on SPR phase detection by simulated annealing particle swarm optimization*, Optics Communications **430** (2019) 238.

[79] R.I. Rabady and A. Ababneh, *Global optimal design of optical multilayer thin-film filters using particle swarm optimization*, Optik **125** (2014) 548.

[80] Z.-H. Ruan, Y. Yuan, X.-X. Zhang, Y. Shuai and H.-P. Tan, *Determination of optical properties and thickness of optical thin film using stochastic particle swarm optimization*, Solar Energy **127** (2016) 147.

[81] A. Mehmood, A. Zameer, M.A.Z. Raja, R. Bibi, N.I. Chaudhary and M.S. Aslam, *Nature-inspired heuristic paradigms for parameter estimation of control autoregressive moving average systems*, Neural Computing and Applications **31** (2019) 5819.

[82] Y. Yetis and M. Jamshidi, *Forecasting of Turkey's electricity consumption using Artificial Neural Network*, .

[83] I.M. Yassin, A. Zabidi, M.S. Amin Megat Ali, N. Md Tahir, H. Zainol Abidin and Z.I. Rizman, *Binary particle swarm optimization structure selection of nonlinear autoregressive moving average with exogenous inputs (NARMAX) model of a flexible robot*

arm, *International Journal on Advanced Science, Engineering and Information Technology* **6** (2016) 630.

[84] S. Akbar, F. Zaman, M. Asif, A.U. Rehman and M.A.Z. Raja, *Novel application of FO-DPSO for 2-D parameter estimation of electromagnetic plane waves*, *Neural Computing and Applications* **31** (2019) 3681.

[85] A. Stacey, M. Jancic and I. Grundy, *Particle swarm optimization with mutation*, .

[86] R. Eberhart and J. Kennedy, *A new optimizer using particle swarm theory*, .

[87] M. Dey and S. Roy, *A Realistic Neutrino mixing scheme arising from A_4 symmetry*, 2304.07259.

[88] V.V. Vien, A.E. Cárcamo Hernández and H.N. Long, *The $\Delta(27)$ flavor 3-3-1 model with neutral leptons*, *Nuclear Physics B* **913** (2016) 792 [1601.03300].

[89] R.L. Workman, V.D. Burkert, V. Crede, E. Klempt, U. Thoma, L. Tiator et al., *Review of Particle Physics*, *Progress of Theoretical and Experimental Physics* **2022** (2022) 083C01.

[90] M. Katrin Collaboration, Aker, A. Beglarian, J. Behrens, A. Berlev, U. Besserer, B. Bieringer et al., *Direct neutrino-mass measurement with sub-electronvolt sensitivity*, *Nature Physics* **18** (2022) 160.

[91] W. Rodejohann, *Neutrino-Less Double Beta Decay and Particle Physics*, *International Journal of Modern Physics E* **20** (2011) 1833 [1106.1334].

[92] M. Mitra, G. Senjanović and F. Vissani, *Neutrinoless double beta decay and heavy sterile neutrinos*, *Nuclear Physics B* **856** (2012) 26 [1108.0004].

[93] S.M. Bilenky and C. Giunti, *Neutrinoless Double-Beta Decay:. a Brief Review*, *Modern Physics Letters A* **27** (2012) 1230015 [1203.5250].

[94] W. Rodejohann, *Neutrinoless double-beta decay and neutrino physics*, *Journal of Physics G Nuclear Physics* **39** (2012) 124008 [1206.2560].

[95] J.D. Vergados, H. Ejiri and F. Šimkovic, *Theory of neutrinoless double-beta decay*, *Reports on Progress in Physics* **75** (2012) 106301 [1205.0649].

[96] H. Ishimori, T. Kobayashi, H. Ohki, H. Okada, Y. Shimizu and M. Tanimoto, *An Introduction to Non-Abelian Discrete Symmetries for Particle Physicists*, vol. 858, Springer (2012), 10.1007/978-3-642-30805-5.